Profile Drag and Wake Momentum Deficit

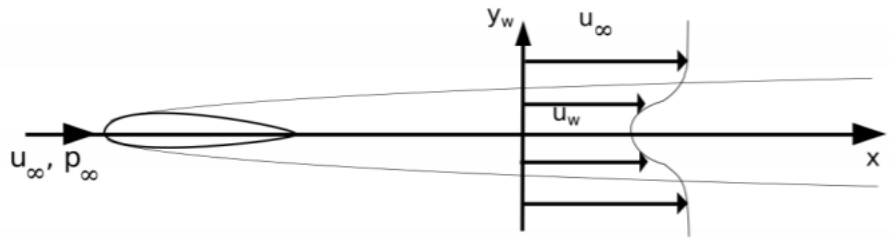

Group 8

Date of experiment: 21 February 2019

Members: Lewis McDonald

Xerxes Chong Xian

Rutvik Badkas

Leo Bugeja

Elizabeth Lingkan

Liao Zijun

Abstract

This experiment obtains the contributions of skin friction and pressure drag to the overall profile drag of a NACA0015 aerofoil tested at a $0°$ angle of attack and a freestream velocity of $37.44 m/s$. The aerofoil had a chord length of $15.24 cm$ and was tested in a $50.8 cm$ wind tunnel. Pressure readings were measured from 2 multi-tube manometers. Pressure drag was obtained empirically using surface pressure readings from 16 tappings on the surface of the aerofoil. The profile drag was obtained empirically from 18 pitot tubes mounted in the wake, downstream of the aerofoil. Experimental results were in-line with theory, confirming the dominance of skin-friction contribution over pressure drag in streamlined objects like an aerofoil. Pressure drag contributed 46% while skin friction contributed 54% to the profile drag. Sources of errors responsible for deviation of values were presented and discussed.

Objectives

The main objective of this experiment was to obtain the experimental contributions of the skin and pressure drag to the overall profile drag of a NACA0015 aerofoil. These values were also compared to theoretical values obtain with the XFoil program. The flow conditions are shown in Table 1.

Table 1. Flow conditions

Freestream Velocity (m/s)	Temperature (℃)	Mach No.	Dynamic Viscosity (Ns/m^2)	Reynolds Number
37.44	26.2	0.108	18.4×10^{-6}	0.367×10^{6}

Results

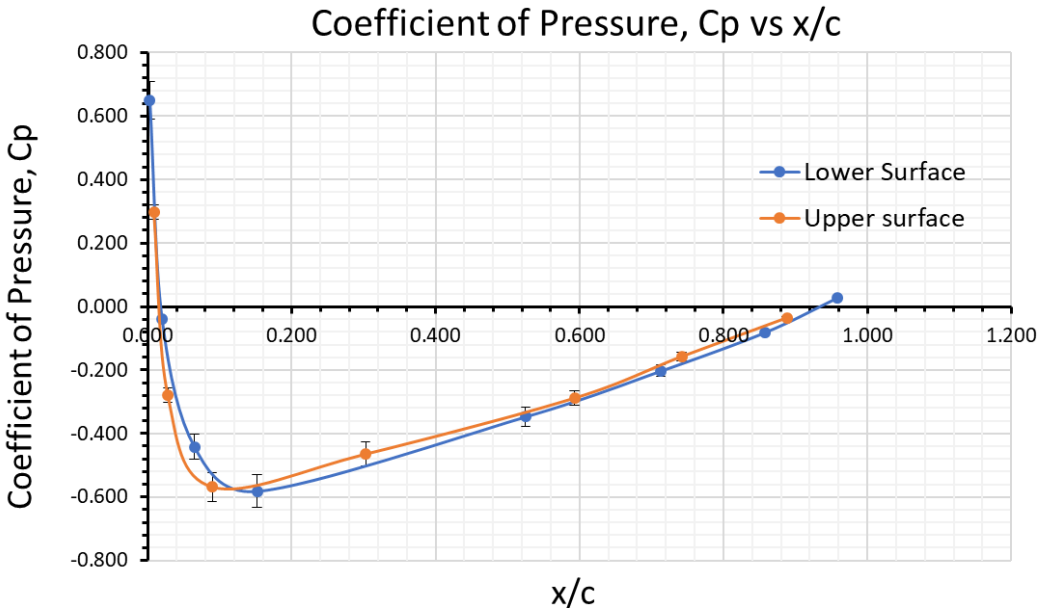

Figure 1. Plot of Cp vs x/c for the upper and lower surface

From Figure 1, the pressure distribution of the upper and lower surface does not completely coincide but are close to each other. This contradicts the assumption that the angle of attack of the aerofoil was set at 0°. An unequal pressure distribution between upper and lower surface of an aerofoil generates lift, evaluated using the formula (1) below;

$$C_L = \frac{1}{c}\int_0^c (C_{P,Upper} - C_{P,Lower})\, d(x)$$

$C_{P,Upper}$ and $C_{P,Lower}$ are the coefficients of pressure along the points on the upper and lower surface of the aerofoil respectively. The integration was performed between 0 and the chord length, c. Implementing a trapezoidal numerical integration method using the "trapz" function on MatLab, the approximated Coefficient of Lift = -0.0224. As this angle is assumed to be small, the true angle of attack of the aerofoil was obtained using the equation $C_L = 2\pi\alpha$, where α is the angle of attack of the aerofoil. α was found to be $-0.204°$. This small angle of attack is a source of error that will be elaborated upon under error analysis.

The pressures close to the trailing edge fails to recover to that of the leading edge. This suggest losses of the flow and is in fact, characteristic of viscous flows.

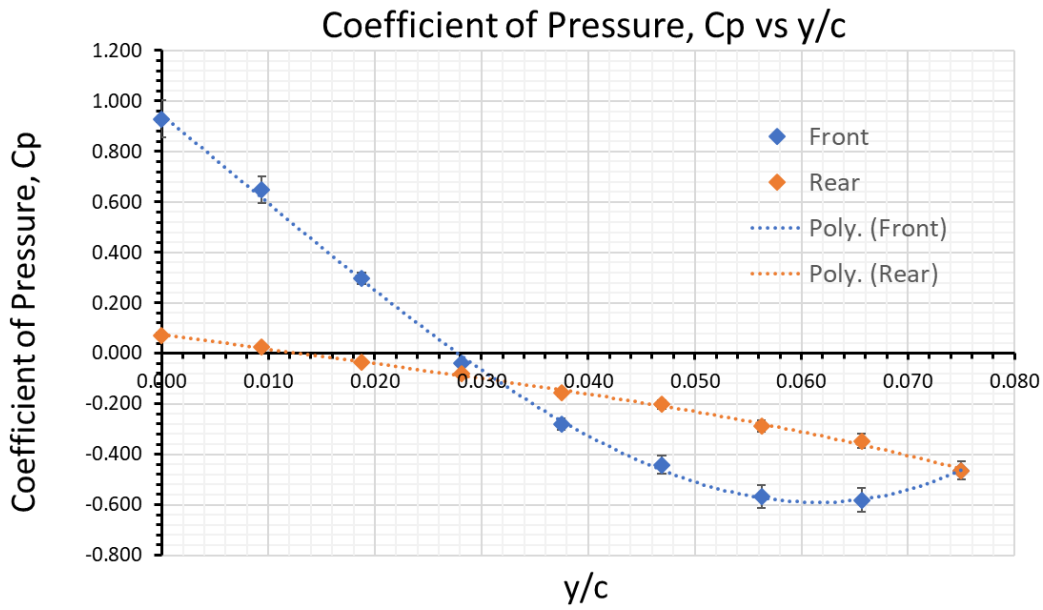

Figure 2. Plot of Cp vs y/c for the front and rear of the aerofoil

From Figure 2, the Coefficient of Pressure Drag, C_{Dp} can be found using the Equation 1 of the handout (1), which evaluates the difference in areas bounded by the curves of the upper and lower surface with respect to the x-axis of Figure 2 . The integration was performed between 0 and Y, where Y represents the maximum thickness of the aerofoil (normalised by chord length, c). Once again, the trapz() function was utilised to numerically obtain $C_{Dp} = 0.00426 \pm 0.00105$.

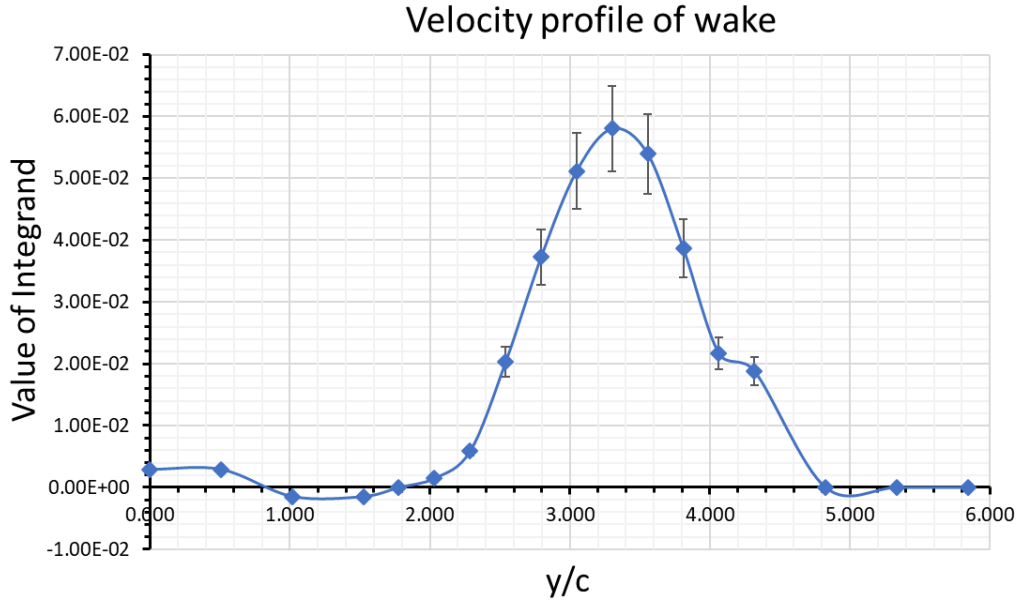

Figure 3. Plot of the integrand of Equation 2 vs y/c. This represents the velocity profile of the wake

Similarly, using Equation 2 of the handout (1), the Coefficient of Profile Drag is found to be $C_D = 0.00934$. The assumption is made that only skin friction, C_{Df} , and pressure drag, C_{Dp}, are contributors to profile drag. As the Mach Number is much lower than sonic conditions (0.108<1), wave drag is assumed to not exist.

The XFoil program was utilised to obtain a set of drag coefficients for a NACA0015 aerofoil at similar flow conditions to Table 1, the plots and values of which can be found in Figure A.1 and Figure A.2 of the Appendix.

Error Analysis

Small angle of attack

A small angle of attack of $-0.204°$ introduced lift-induced drag. This is a pressure force which acts parallel and opposite to the direction of motion, contributing to the net pressure drag force, resulting in a larger pressure drag compared to a $0°$ angle of attack (2).

Effect of blockage

The blockage effects must be considered when the dimensions of the test specimen are large relative to the test section. This effect is a local increase in the velocity of the test section, causing lower than normal readings from the pressure tappings on the aerofoil, which leads to higher local Cp and thus a higher Coefficient of Pressure Drag recorded. As the free stream Mach number is lower than 0.3 (1), compressibility effects can be ignored and applying mass continuity across the wind tunnel results in a higher velocity at the test section. A blockage ratio of > 0.03 requires the application of correction equations (3). This NACA0015 has chord of 0.1524m with a maximum thickness of 15% of its chord length, which equates to 0.0231m. With a 50.8cm working section of the wind tunnel, the blockage ratio is $\frac{0.0231}{0.508} = 0.045$. Hence, blockage equations should have been applied to the experimental data.

Error propagation

The manometer had a smallest division of 0.2cm and thus the readings had an absolute uncertainty of $\varepsilon(l) = \pm 0.001\text{m}$ and the manometer tilting angle had an uncertainty of $\varepsilon(\theta) = \pm 0.5°$. The absolute error in the calculated vertical liquid height at each tapping was calculated as such: $\varepsilon(h)_n = h_n\left(\frac{0.001}{l_n} + \frac{0.5\cos\theta}{\theta}\right)$. The absolute error of the calculated pressure differential at each tapping was found by:

$$\varepsilon(\Delta p)_n = \rho g\,(\varepsilon(h)_\infty + \varepsilon(h)_n) \qquad \varepsilon\left(C_p\right)_n = \frac{\varepsilon(\Delta p)_n}{0.5\rho V_\infty^2}.$$

Finally, the absolute errors associated with each integrand was calculated and summed up to obtain the final error of the calculated pressure drag coefficient which was found to be $\varepsilon(C_{D_p}) = \pm 0.00105$ or a percentage error of 17.8%.

As the theory implemented in calculating the pressure drag coefficient assumed a symmetrical wing at zero angle of incidence, the accuracy of the final value would have been affected by any deviation in the model's incidence that gives a pressure distribution that was not exactly symmetrical. Additionally, during the experiment, the ambient temperature was found to increase by a few degrees due to the heating of the wind tunnel motor. This could have affected values of density used in the calculations which decreases the accuracy of the final value. This could also have changed the Reynolds Number, making the input values into XFoil incorrect.

Discussion

Skin friction is generated from the shear stresses that act tangential and opposite to the direction of motion, decreasing the velocity of the fluid elements. It is pronounced in the boundary layer, where the combination of the "no-slip" condition at the surface and viscosity

produces a large velocity gradient. Skin friction increases with Reynolds Numbers. However, this effect is often negligible in regions of flow far from the boundary layer, which are assumed to be inviscid.

Pressure drag is caused by regions of separated flow. Fluid elements in the boundary layer, lacking the velocity (and hence the momentum) to overcome the adverse pressure gradient, eventually come to a stop and reverse in direction, causing the flow to separate. Pressure acts normal to the surface and its distribution give rise to vertical and horizontal forces, corresponding to the lift and pressure drag forces respectively. Without flow separation, the pressure force on the rear balances out that acting on the front. With flow separation, the rear pressure force is smaller than the front pressure force, causing a net pressure force in the direction opposite of motion. The larger the area of separated flow, the smaller the rear pressure force and the larger the net pressure drag. An aerofoil at increasing angles of attack shifts the separation point forwards, increasing the wake size and hence, increasing pressure drag. Hence, a $0°$ angle of attack should see pressure drag at a minimal and skin friction dominate.

Table 2. Experimental and XFoil values with deviation

	Experimental	XFoil	Deviation
Coefficient of Pressure Drag, C_{Dp}	$4.26 \times 10^{-3} \pm 0.00105$	2.88×10^{-3}	11.5 – 84.4%
Coefficient of Skin Friction, C_{Df}	5.08×10^{-3}	5.20×10^{-3}	2.31%
Coefficient of Profile Drag, C_D	$9.34 \times 10^{-3} \pm 0.00224$	8.07×10^{-3}	12.0 – 43.5%

From Table 2, pressure drag contributed 46% while skin friction contributed 54% to the profile drag. A large deviation is evident in experimental pressure drag and those obtained with XFoil. This large deviation resulted in the deviation of values for the Profile Drag as well. This can be attributed to propagation of errors from the measuring equipment and blockage effects. The small angle of attack introduced lift-induced drag and increased the wake size, increasing pressure drag. The XFoil program uses potential flow theory and boundary layer integration to evaluate flow around a 2D aerofoil. The possible 3D effects of an aerofoil in a wind tunnel, such as lift-induced drag and blockage effects were not accounted for and could have contributed to the deviation. Lastly, the limited number of pressure readings of the surface combined with the numerical method utilised inevitably introduced errors in the integration. Using more pressure tapping (ideally an infinite number) will produce more accurate distributions of pressure and hence more accurate numerically-obtained coefficients.

Despite the deviation of values, the experimental agree with theory, showing the dominance of skin friction over pressure drag for the streamlined body of the NACA0015 aerofoil at $0°$.

Conclusion

For the streamlined body of the NACA0015 aerofoil tested at a $0°$ angle of attack and a free stream velocity of $37.44 m/s$, the postulation of skin friction being the dominating profile drag component was confirmed by the experimental results, having contributed 54%. Despite the large range of deviation between XFoil and experimental values of pressure drag, sources of error related to the wind-tunnel testing of a 3D aerofoil, such as the; blockage effect, small angle of attack and lift-induced drag, uncertainties of the measuring equipment as well as the limitations of the XFoil program could have contributed to this deviation.

Bibliography

1. **Papadakis, Dr George.** *Module AE2-214 - Experimental Methods: Profile Drag and Wake Momentum Deficit.* Aeronautics, Imperial College London. London : Department of Aeronautics, Autumn Term 2018. Laboratory Handout.
2. **John D.Anderson, Jr.** *Fundamentals of Aerodynmics, Fifth Edition.* [ed.] McGraw-Hill. s.l. : McGraw-Hill Series in Aeronautical and Aerospace Engineering, 2011.
3. **Anthoine, J., Olivari, D. and Portugaels, D.** *DRAG COEFFICIENT DETERMINATION OF BLUFF BODIES –*. von Karman Institute for Fluid Dynamics. Rhode Saint Genèse, Belgium : von Karman Institute for Fluid Dynamics, May 2004. Scientific Paper.

Appendix

Flow conditions and other constants

Table A.1 Experimental constants assumed

Ethanol Density (kg/m^3)	Air Density (kg/m^3)	$P_{atmosphere}$ (kPa)
789	1.225	102.5

Raw data for obtaining Pressure Drag Coefficient

Table A.2 Static and total pressure and the inclination of Manometer 1

Manometer 1 Inclination (°)	Static Pressure (cm)	Total Pressure (cm)
30	29.4	8.7

Table A.3. Coordinates of the 16 surface tappings on the aerofoil. The point in red and bold is the origin. The respective manometer readings and the adjusted heights are also shown

Hole	x/c	y/c	Manometer Height (cm)	Actual Height (m)
1	0.958	0.009	28.8	0.144
3	0.858	0.028	31.2	0.156
5	0.713	0.047	33.9	0.170
7	0.525	0.066	37.1	0.186
9	0.152	0.066	42.3	0.212
11	0.065	0.047	39.2	0.196
13	0.020	0.028	30.3	0.152
15	0.003	0.009	15.0	0.075
16	**0.000**	**0.000**	8.8	0.044
2	0.888	0.019	30.2	0.151
4	0.742	0.038	32.9	0.165
6	0.593	0.056	35.8	0.179
8	0.303	0.075	39.7	0.199
10	0.090	0.056	42.0	0.210
12	0.028	0.038	35.6	0.178
14	0.009	0.019	22.8	0.114

Table A.4 Cp values evaluated using trapz to obtain pressure drag. Point in red and bold is the y-intercept added to close the Cp vs y graph

Hole	y (m)	Cp
-	**0**	**0.072**
1	0.0014	0.027
2	0.0029	-0.036
3	0.0043	-0.081
4	0.0057	-0.158
5	0.0071	-0.203
6	0.0086	-0.288
7	0.0100	-0.347
8	0.0114	-0.464
9	0.0100	-0.581
10	0.0086	-0.568
11	0.0071	-0.442
12	0.0057	-0.279
13	0.0043	-0.041
14	0.0029	0.297
15	0.0014	0.649
16	0.0000	0.929

Raw data for obtaining Profile Drag Coefficient

Table A.5 Static and total pressure and the inclination of Manometer 2

Manometer 2 Inclination (°)	Static Pressure (cm)	Total Pressure (cm)
20	46.7	12.9

Table A.6 Points in red and bold were used in the numerical integration to obtain the profile drag

Pitot	Distance (cm)	Integrand
1	0.000	2.92E-03
3	0.508	2.92E-03
5	1.016	-1.46E-03
7	1.524	-1.46E-03
8	1.778	1.33E-15
9	2.032	1.46E-03
10	2.286	5.83E-03
11	**2.540**	**2.03E-02**
12	**2.794**	**3.73E-02**
13	**3.048**	**5.12E-02**
14	**3.302**	**5.80E-02**
15	**3.556**	**5.39E-02**
16	**3.810**	**3.87E-02**
17	**4.064**	**2.17E-02**
18	**4.318**	**1.88E-02**
20	4.826	1.33E-15
22	5.334	1.33E-15
24	5.842	1.33E-15

XFoil plot and data

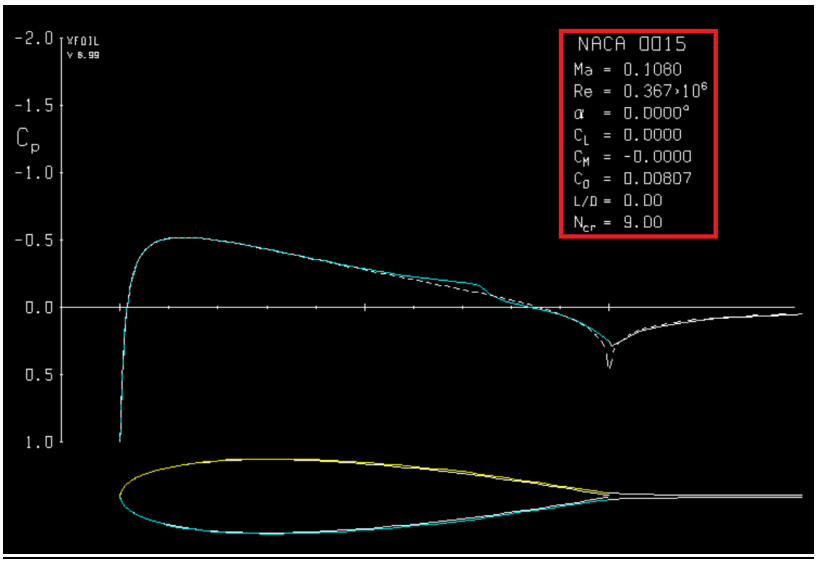

Figure A.1 XFoil plot of the NACA0015 with similar flow conditions

```
Side 1  free  transition at x/c =  0.7294   65
Side 2  free  transition at x/c =  0.7293   65

  1   rms: 0.8007E-06   max: 0.6678E-05   C at   65  2
      a =  0.000      CL =  0.0000
     Cm = -0.0000     CD =  0.00807   =>   CDf =  0.00520    CDp =  0.00288
```

Figure A.2 From left to right, the XFoil values of Coefficient of Drag, Coefficient of Skin Friction and Coefficient of Pressure Drag are highlighted in the red box